# Maximizing Revenue with Adaptive Modulation and Multiple FECs in Flexible Optical Networks

Cao Chen, Fen Zhou, *Senior Member, IEEE*, Massimo Tornatore, *Senior Member, IEEE*, Shilin Xiao

***Abstract*—Flexible optical networks (FONs) are being adopted to accommodate the increasingly heterogeneous traffic in today's Internet. However, in presence of high traffic load, not all offered traffic can be satisfied at all time. As carried traffic load brings revenues to operators, traffic blocking due to limited spectrum resource leads to revenue losses. In this study, given a set of traffic requests to be provisioned, we consider the problem of maximizing operator's revenue, subject to limited spectrum resource and physical layer impairments (PLIs), namely amplified spontaneous emission noise (ASE), self-channel interference (SCI), cross-channel interference (XCI), and node crosstalk. In FONs, adaptive modulation, multiple FEC, and the tuning of power spectrum density (PSD) can be effectively employed to mitigate the impact of PLIs. Hence, in our study, we propose a universal bandwidth-related impairment evaluation model based on channel bandwidth, which allows a performance analysis for different PSD, FEC and modulations. Leveraging this PLI model and a piecewise linear fitting function, we succeed to formulate the revenue maximization problem as a mixed integer linear program. Then, to solve the problem on larger network instances, a fast two-phase heuristic algorithm is also proposed, which is shown to be near-optimal for revenue maximization. Through simulations, we demonstrate that using adaptive modulation enables to significantly increase revenues in the scenario of high signal-to-noise ratio (SNR), where the revenue can even be doubled for high traffic load, while using multiple FECs is more profitable for scenarios with low SNR.**

***Index Terms*—Flexible optical networks (FONs), revenue maximization, adaptive modulation, multiple forward-error correction (FEC).**

## I. Introduction

ACCORDING to recent traffic reports, network traffic (fueled by successful network services like video on demand, file sharing, online gaming, and video conferencing) is still growing exponentially in today's Internet [2]. This constant traffic growth can be accommodated by novel flexible optical networks (FONs) which can support large transmission capacity. As busy hour traffic peaks are expected to increase almost 5 times between 2017 and 2022 (average Internet traffic will increase only 3.7 times), the problem of coping with sudden resource crunches will become even more a matter of concern in next years, especially during peak usage periods [2]–[5]. During resource crunch, given the limited spectrum resources in FONs, not all traffic requests can be fully satisfied and some traffic must be blocked. As carried traffic brings revenue to operators, resource crunch events can lead to significant revenue losses for operators. Hence, efficient provisioning strategies in optical networks are required to reduce blocking and maximize operators' revenue.

In FONs, an adequate amount of spectrum resources to establish a lightpath is required for each request. Since FONs can support variable routes, bandwidth, and modulation formats (MFs), the routing and wavelength assignment problem has evolved into the routing and spectrum assignment [6]. However, since the spectral-efficiency granularity of $m$-ary quadrature amplitude modulation ($m$QAM) is coarse, the available spectrum resources might not be most-effectively utilized, resulting in the stranded capacity and loss in services' revenue. Hence, to achieve even higher resource-allocation flexibility that granted by multiple MFs, tunability of forward error-corrections (FECs) has been introduced to adjust the spectral efficiency [7]. It can be typically observed that overhead ratios range values from 7% to 20%. The combination of MF and FEC, referred to as *transmission mode* in this paper, can provide more candidate choices in terms of spectral efficiency and transmission reach. Compared to the traditional approaches aiming at revenue improvement, such as using backup lightpaths for living traffic [8] or upgrading to multi-core fibers [9], using MF and FEC is more efficient and faster. The traffic provisioning with multiple MFs and FECs maps into a problem of routing, MF, FEC, and spectrum assignment [10]. While the optimal combination of MF and FEC has been investigated at the transmission layer in, *e.g.*, [11, 12], in this paper we investigate how the combination of MF and FEC can be used to maximize revenues through appropriate traffic provisioning strategies.

To support multiple MFs and FECs in FONs, traffic provisioning strategies must be cross-layer [13], *i.e.*, they must be capable of taking in account physical layer aspects, to achieve efficient spectrum usage. The physical layer impairments (PLIs) of a lightpath are influenced by the bandwidth, by power spectral densities (PSDs), by the route length, and by the number of crossed nodes. Due to the impact of all the parameters just mentioned, the quality of transmission (QoT)

This work was supported in part by the Campus France Eiffel Scholarship under Grant No. 895145D, in part by the China Scholarship Council under Grant No. 201806230093, in part by the National Natural Science Foundation of China under Grant No. 62071295, and in part by the National Science Foundation under Grant No. 1716945. A preliminary version of this work was presented as a short paper at IEEE HPCC 2019 [1]. (*Corresponding author: Fen Zhou*)

Cao Chen is with the State Key Laboratory of Advanced Optical Communication Systems and Networks, Shanghai Jiao Tong University, Shanghai, 200240, China, and also with the CERI-LIA in University of Avignon, France (email: cao.chen@alumni.univ-avignon.fr).

Fen Zhou is with the Computer Science Laboratory, University of Avignon, Avignon 84000, and also with the IMT Nord Europe, Institut Mines-Télécom, University of Lille, Center for Digital Systems, F-59000 Lille, France (email: fen.zhou@univ-avignon.fr).

Massimo Tornatore is with the Department of Electronics, Information and Bioengineering in Politecnico di Milano, Italy (email: massimo.tornatore@polimi.it).

Shilin Xiao is with the State Key Laboratory of Advanced Optical Communication Systems and Networks, Shanghai Jiao Tong University, Shanghai, 200240, China (email: slxiao@sjtu.edu.cn).

(*e.g.*, expressed by lightpath's Signal to Noise Ratio, SNR) may degrade and fall below acceptable threshold for correct signal reception after a long distance. Recent studies on the node crosstalk have considered the wavelength-related and frequency slot-related crosstalk component [14, 15]. However, current studies overestimate the PLIs with the assumption of full wavelength or full consecutive frequency slots for each lightpath. For example, the node crosstalk on provisioned bandwidth of 12.5 GHz slot is greater than the actual value of the sub-channel bandwidth with 6.25 GHz [16]. To reduce the PLIs, a guard band (*e.g.*, 12.5 GHz) may be used, but incurring in inefficient usage of spectrum resources. Therefore, the PLI model that we propose is based on the channel bandwidth, which means that the impairments of node crosstalk and fiber nonlinear interference are evaluated by the value of actual channel bandwidth occupied by a signal rather than a wavelength or slot, which ensures that the PLIs are properly estimated and spectrum resource is effectively utilized.

The main novelty and contributions of this paper can be summarized as follows:

1) We devise novel traffic provisioning strategies to maximize the total revenue using different MF and FEC configurations. The lightpaths can adopt transmission mode with either higher spectral efficiency or longer transmission reach to guarantee the bit-rate under resource crunch. Compared to single MF or single FEC, the combination can provide just-enough spectral efficiency thus improve the traffic provisioning. By using a piecewise linear fitting to model the nonlinear interference and calculating the crosstalk of intermediate nodes, we linearize the PLIs then model the studied problem as a mixed integer linear program (MILP). Our MILP model is based on flow rather than pre-calculated route. Without using the candidate route, our method can get the optimal solution irrespective of the number of routes.
2) We propose a novel lightpath's PLI evaluation model based on the channel bandwidth that incorporates the impact of different PSDs, FECs, and MFs. By tracing the relationship between the PSD and SNR, we observe that using MFs enables to increase revenues with high SNR, while using multiple FECs is preferred for the scenarios of low SNR. Besides, unlike the method that evaluates PLIs through the assigned wavelengths or frequency slots, the bandwidth-related method evaluates the PLIs through its actual channel bandwidth on continuous spectrum resources, which allows describing the PLIs of an optical signal at an arbitrary bandwidth.
3) A fast and near-optimal heuristic algorithm is also proposed to solve the revenue maximization problem.

### A. Related Works

Previous studies have been conducted to increase the network revenue from various perspectives (*e.g.*, by flexible bandwidth allocation [3], by flexible availability targets [8], etc.). In [3], the request's acceptable bandwidth is assumed as a bandwidth interval. A request could be accepted either at the high bandwidth with higher revenue, or at the low bandwidth with lower revenue. Using this strategy, they optimized the bandwidth and route to increase network revenue. In [8], a new incoming request can be admitted by setting the service downtime for several requests but without violating its service level agreement such that the net revenue (revenue after the penalty) could be maximized. Unlike these works [3, 8], our study makes use of the benefits of improved spectral efficiency to increase network revenue.

Resource allocation in optical networks is evolving to incorporate the increased flexibilities of coherent transmission and its resulting improved spectrum efficiency. In [6], the route and spectrum assignment was initially formulated, using an optimal integer linear programming (ILP) formulation and a decomposition approach. Incorporating the MF flexibility, the advanced resource allocation problem of route, modulation format, and spectrum assignment has been studied [17], where benefits in terms of spectrum savings are evaluated. By using MF and FEC, several other lightpath provisioning models have been studied targeting different network performance metrics, such as energy saving [7], bandwidth saving [12], etc. However, these models working on the assumption that all requests are equally accepted neglect the differentiated requirements (*e.g.*, availability, service types, priorities, distance, service type, etc.) of requests, which might result in lower efficiency in collecting revenues. In order to maximize the total accepted revenue, we devise a novel traffic provisioning strategy and leverages adaptive MFs and multiple FECs.

Besides, we incorporate improved PLI modeling to improve the decision-making process for the selection of MF and FEC. In fact, to properly capture increased flexibility in using spectrum resources, the classical PLI models have to be evolved and incorporated into the design models and algorithms. In WDM networks, a PLI model capturing the node crosstalk and nonlinear interference was proposed in [15] considering the impact of interfering wavelengths on common links, or the interference of the same wavelength used by other lightpaths on common nodes. Since the introduction of the Gaussian Noise (GN) model and other low-complexity approaches (as in [18]), the evaluation of fiber nonlinear interference became possible in FONs where an optical signal can be characterized by arbitrary signal bandwidths, spectrum positions, and PSDs. The PLI models capturing both nonlinear interference [19] and node crosstalk [14] have been used in practical deployments. However, these PLI models are based on the assumption that signal bandwidth is approximated as multiple of discrete frequency slots [14, 15, 19]. They are unable to evaluate the PLIs depending on the actual signal bandwidth (or baud-rate), and hence cannot capture the effect as the filter narrowing effect, the transceiver noise, the in-band node crosstalk, etc. Using a channel-based evaluation, the study in [20] focused for the first time on the nonlinear interference modeling, and our previous study [21] focused on both the nonlinear interference and transceiver noise. Unlike [20, 21], this paper, for the first time to the best of our knowledge, models the PLIs (namely, nonlinear interference and node crosstalk) using the channel bandwidth. Besides, this model allows for the analysis of signal quality considering different MFs, FECs, and PSDs.

The rest of this paper is organized as follows. We describe

our proposed PLI model in Sec. II. The problem of traffic provisioning with adaptive MFs and multiple FECs is stated in Sec. III. To solve it, we present an MILP model in Sec. IV and a heuristic algorithm in Sec. V. Illustrative numerical results are presented in Sec. VI. Finally, Sec. VII concludes this paper.

## II. Physical Layer Model

In this section, we discuss our proposed PLI evaluation model. We also include a description of the signal impairments and of the optical transmission.

### A. MF and FEC

We denote as transmission mode $\mathcal{C}$ the combination set of MF and FEC, $\mathcal{C}$=($\mathcal{M}$,$\mathcal{F}$). For an arbitrary transmission mode $c \in \mathcal{C}$, its spectral efficiency is

$$SE(c) = SE(m, f) = m/(1 + OH_f) \tag{1}$$

where $m$ is the theoretically maximum spectral efficiency of the MF, and $OH_f$ is the FEC overhead ($\times$100%). The spectral efficiency and SNR threshold of the example transmission mode in this paper are shown in Fig. 1, where we assume four available polarization-multiplexing MFs (PM-BPSK, PM-QPSK, PM-8QAM, and PM-16QAM) and six FEC OHs (1%, 7%, 10%, 20%, 30%, and 50%). For example, the spectral efficiency of PM-16QAM with FEC OHs 10% is 8/(1+10%)=7.27 bit/s/Hz, while the SNR threshold is 12.25 dB. To satisfy QoT, the SNR should be over the threshold for each transmission mode. Next, we present the PLI model that impacts SNR.

### B. PLIs Model

When an optical signal propagates, it suffers diverse forms of PLIs, including white Gaussian noise amplified spontaneous emission (ASE), self-channel interference (SCI), and cross-channel interference (XCI) [18]. Both SCI and XCI are caused by the Kerr effect of fiber, which can be estimated as additive white Gaussian noise by the GN model [22]. When a signal traverses an optical cross-connect (OXC), the node crosstalk from signal adding or dropping (AD) at node must be also considered [13, 14].

Next, we describe these impairments by using the signal's PSD and bandwidth. The PLI related parameters are given in Table I. We note $c_i$ as the transmission mode used by request $i$. $\text{SNR}_i$ denotes its received signal-to-noise ratio, and $\text{SNR}^{\text{th}}_{c_i}$ is the SNR threshold for $c_i$. By summing up all noise contributions due to PLIs, a request $i$ can be served if it satisfies the QoT constraint as in (2).

$$\text{SNR}_i = \frac{G_i}{G_i^{\text{ASE}} + G_i^{\text{SCI}} + G_i^{\text{XCI}} + G_i^{\text{AD}}} \geq \text{SNR}^{\text{th}}_{c_i} \tag{2}$$

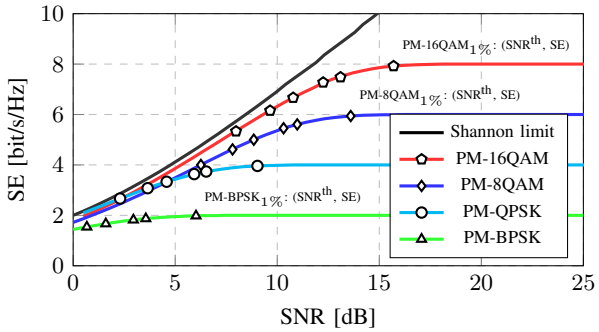


| MF | $m$ | FEC | | | | | |
|---|---|---|---|---|---|---|---|
| | | OH=1% | OH=7% | OH=10% | OH=20% | OH=30% | OH=50% |
| PM-BPSK | 2 | 6.02 | 3.56 | 2.95 | 1.6 | 0.67 | - |
| PM-QPSK | 4 | 9.03 | 6.52 | 5.93 | 4.58 | 3.65 | 2.3 |
| PM-8QAM | 6 | 13.6 | 10.98 | 10.31 | 8.85 | 7.81 | 6.26 |
| PM-16QAM | 8 | 15.7 | 13.1 | 12.25 | 10.78 | 9.65 | 7.98 |

Fig. 1. The maximum achievable spectral efficiency of different transmission modes with different SNRs [23, 24]. The SNR threshold for each marker is illustrated in the table below the figure.

TABLE I
Parameters for PLIs

| Parameters and description | |
|---|---|
| $\alpha$ | Power attenuation ratio of fiber, 0.2 dB/km. |
| $\beta_2$ | Second order dispersion of 1550nm wavelength, -21.7 ps$^2$/km. |
| $\gamma$ | Non-linear coefficient, 1.3 (W·Km)$^{-1}$. |
| $h$ | Planck's constant. |
| $\nu$ | Frequency of optical signal, 192.5 THz. |
| $\mu$ | $3\gamma^2/(2\pi\alpha\beta_2)$. |
| $\rho$ | $\pi^2\beta_2/\alpha$. |
| $\epsilon_{\text{X}}$ | OXC port leakage ratio, -25 dB. |
| $n_{\text{sp}}$ | Noise figure of optical amplifier, 7dB. |
| $G_i$ | Power spectral density of request $i$. |
| $G_i^{\text{ASE}}$ | PSD of ASE. |
| $G_i^{\text{SCI}}$ | PSD of SCI. |
| $G_i^{\text{XCI}}$ | PSD of XCI. |
| $G_{ijv}^{\text{AD}}$ | PSD of AD node crosstalk from $j$ to $i$ on the common node $v$. |
| $G_i^{\text{AD}}$ | PSD of AD, $G_i^{\text{AD}} = \sum_{jv} G_{ijv}^{\text{AD}}$. |
| $\text{SNR}_c^{\text{th}}$ | SNR threshold of transmission mode $c$. |
| $L_{\text{span}}$ | Span length, 100 km/span. |

For ease of the MILP modeling, we can also express (2) in its reciprocal form,

$$\begin{cases} \dfrac{1}{\text{SNR}_i} = t_i^{\text{ASE}} + t_i^{\text{SCI}} + t_i^{\text{XCI}} + t_i^{\text{AD}} \leq \dfrac{1}{\text{SNR}^{\text{th}}_{c_i}} \\ t_i^{\text{ASE}} = G_i^{\text{ASE}}/G_i \\ t_i^{\text{SCI}} = G_i^{\text{SCI}}/G_i \\ t_i^{\text{XCI}} = G_i^{\text{XCI}}/G_i \\ t_i^{\text{AD}} = G_i^{\text{AD}}/G_i \end{cases} \tag{3}$$

where $t_i^{\text{ASE}}$, $t_i^{\text{SCI}}$, $t_i^{\text{XCI}}$, and $t_i^{\text{AD}}$ are the noise to signal ratios of ASE, SCI, XCI, and AD node crosstalk, respectively. The noise to signal ratios can be regarded as the amount of PLIs of ASE, SCI, XCI, and node crosstalk. The detailed computation will be explained next.

*1) Impairments along Fibers (ASE, SCI, and XCI):* ASE noise is a white noise, whose intensity is proportional to the

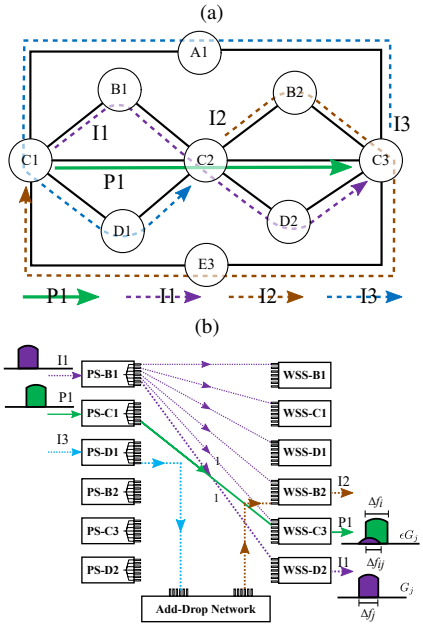


Fig. 2. (a) The 9-node network used to illustrate different forms of AD node crosstalk, (b) Illustration of node crosstalk at node C2 considering a B&S architecture [26]. PS: power splitter (PS).

number of fiber spans and signal bandwidth. In ignoring the factor of bandwidth, its PSD can be expressed by

$$G_i^{\text{ASE}} = N_{\text{span}}(e^{\alpha L_{\text{span}}} - 1)n_{\text{sp}}h\nu \tag{4}$$

where $N_{\text{span}}$ is the number of spans (see Table I for the other parameters).

In GN model, both SCI and XCI are regarded as additive white noise, whose PSD is related to the light power, bandwidth and center frequency. We use (5) and (6) to calculate the PSD of SCI and XCI [18, 25].

$$G_i^{\text{SCI}} = N_{\text{span}}\mu G_i^3 \text{asinh}(\rho \Delta f_i^2) \tag{5}$$

$$G_i^{\text{XCI}} = \sum_j N_{\text{span},ij}\mu G_i G_j^2 \ln\left(\frac{|f_i - f_j| + \Delta f_j/2}{|f_i - f_j| - \Delta f_j/2}\right) \tag{6}$$

where $\Delta f_i$ is the bandwidth of request $i$, and $f_i$ is the relative carrier center frequency. Note that the accuracy in (5) and (6) is only validated in the case where $\Delta f_i \geq 28$ GHz [18], which determines our bit-rate setting in the simulations.

*2) Impairments at Nodes:* Impairments at nodes come from node crosstalk. Only in-band crosstalk is considered in this paper, *i.e.*, the lightpath experiences node crosstalk if it is exposed to the other lightpaths with the overlapping bandwidth. As an example, we use 9-node network in Fig. 1(a) to illustrate the different node crosstalk components. The primary signal P1 is added at node C1, passes through node C2, and is dropped at node C3. Other three crosstalk signals I1, I2, and I3, are also depicted. At each of its nodes (C1, C2 and C3), P1 the primary signal will experience all forms of crosstalk, *i.e.*, adding, passing through, and dropping.

To analyze the node crosstalk, we assume a broadcast-and-select (B&S) OXC architecture for intermediate node C2 [26], as illustrated in Fig. 1(b). It consists of passive optical splitters (PSs) with 1×N ports that broadcast signal copies to the common port at local add/drop side and wavelength selective switches (WSSs) facing different output ports and collecting the signals from add ports. A node crosstalk from signal I1 to P1 arises on WSS-C3 because the broadcast signal I1 is leaked into WSS-C3. We can also observe that the crosstalk signal I3 can leak into P1 on WSS-C3 due to the broadcast function of PS-D1 (the line is not connected in Fig. 2(b) for the sake of visualization). The former node crosstalk from I1 is the passing-through node crosstalk, while the latter from I3 is the dropping node crosstalk. Based on the same analysis, we can also derive other forms of interference at nodes C1 and C3. At node C1, P1 experiences the dropping crosstalk of I2 and the passing-through crosstalk of I3. At node C3, there is no crosstalk, because P1 is dropped locally. In short, the AD node crosstalk exists if primary signal is added at or passing through the node, and crosstalk signal is passing through or dropped at that node.

The amount of node crosstalk depends on the size of the overlapping bandwidth [27]. Unlike the approach in [14] that only supports the node crosstalk by frequency slot, we propose to improve it by adopting the bandwidth, which supports arbitrary bandwidth. Thus, assuming the overlapping bandwidth between the primary signal $\Delta f_i$ and the interfering signal $\Delta f_j$ is $\Delta f_{ij}$, we give the amount of node crosstalk as follows,

$$G_{ijv}^{\text{AD}} = \epsilon_{\text{X}} \Delta f_{ij} G_j \tag{7}$$

where $G_j$ is the PSD of the other interfering signal (for the interference signal $j$ = I1 in the example, $v$ is the node C2, and $\Delta f_{ij} = \left|\frac{\Delta f_i + \Delta f_j}{2} - |f_i - f_j|\right|$).

## III. Traffic Provisioning using MF and FEC in Flexible Optical Networks

We denote an FON by a graph $\text{G}(V, E)$. Each node $v \in V$ represents an OXC. A link $e \in E$ represents two fibers $uv$ and $vu$ $(u, v \in V)$ that carry traffic in opposite directions. Each request $i$ is characterized by its source node $s_i$, destination node $d_i$, bit-rate $r_i$, PSD $G_i$ ($G_i = G$, a constant PSD is assumed for all requests), and revenue level $\eta_i$. The consumed spectrum bandwidth counts $\Delta f_i = r_i/\text{SE}(c_i)$, where $\text{SE}(c_i)$ is the spectral efficiency of transmission mode $c_i$. Normally, the revenue $\eta_i$ is determined by the operator's preference or importance, such as (*i*) time of day, (*ii*) duration, (*iii*) location, (*iv*) distance, (*v*) connection speed, and (*vi*) service type [3]. A random service type parameter is adopted in this paper. Assuming a set of requests in demand list $D$, the total network revenue is the sum of accepted requests' revenue. They might be rejected due to the insufficient spectrum resource, which is limited to $F$ ($F \in \mathbb{R}^+$) on each fiber.

To serve a request, a lightpath should be established on a continuous and contiguous spectrum interval. We indicate the spectrum interval as $[b_i, e_i]$, where $b_i$ and $e_i$ are the beginning and end of the spectrum interval of request $i$, respectively. To satisfy the spectrum continuity and contiguity constraints, the spectrum interval must be the same on all traversed links, and can not overlap with other lightpaths. Due to limited spectrum resources, not all lightpaths can be provisioned. Therefore,

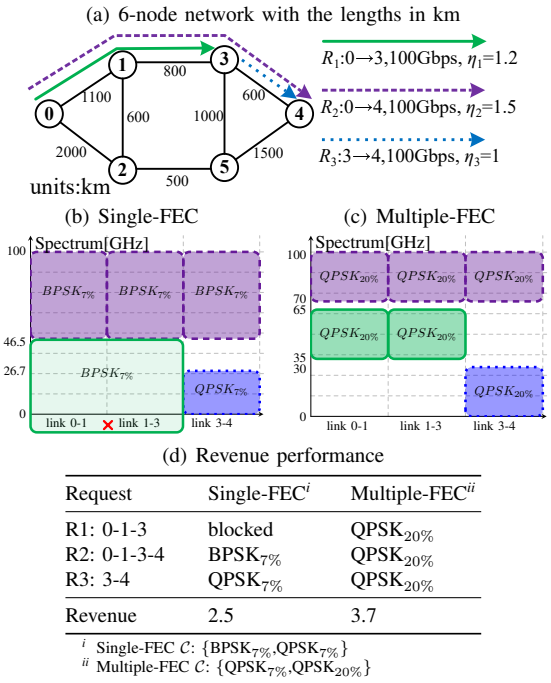


(d) Revenue performance

| Request | Single-FEC[i] | Multiple-FEC[ii] |
|---|---|---|
| R1: 0-1-3 | blocked | $QPSK_{20\%}$ |
| R2: 0-1-3-4 | $BPSK_{7\%}$ | $QPSK_{20\%}$ |
| R3: 3-4 | $QPSK_{7\%}$ | $QPSK_{20\%}$ |
| Revenue | 2.5 | 3.7 |

[i] Single-FEC $\mathcal{C}$: {$BPSK_{7\%}$,$QPSK_{7\%}$}
[ii] Multiple-FEC $\mathcal{C}$: {$QPSK_{7\%}$,$QPSK_{20\%}$}

Fig. 3. Traffic provisioning example with single-FEC and multiple-FEC configurations in 6-node network.

our objective is to maximize the total revenue by optimizing spectrum resource allocation. We use variable $B_i$ to indicate whether request $i$ is served ($B_i = 1$ if it is accepted, 0 otherwise), then the objective function can be expressed by

$$\sum_{i \in D} \eta_i B_i \tag{8}$$

We give an example of revenue difference for different traffic provisioning using transmission mode configurations, *i.e.* single-FEC and multiple-FEC in Fig. 3. Each link has limited spectrum of 100 GHz. The number near each link denotes the length. Three requests R1, R2, and R3 are labeled with source, destination, bit-rate, and revenue. The PSDs for all lightpaths are -11 dBm/GHz.

In single-FEC configuration, FEC OH is fixed at 7%, hence R2 uses $BPSK_{7\%}$ on the channel [46.5, 100], and R3 uses $QPSK_{7\%}$ on channel [0, 26.7]. However, the remaining spectrum [0, 46.5] on link 0-1 is insufficient to support R1 with $BPSK_{7\%}$. Otherwise, if $QPSK_{7\%}$ had been chosen, the QoT of R1 would not have been satisfied because of the fiber nonlinear interference from R2 to R1. Therefore, at most two requests can be accepted with single-FEC configuration, leading to a revenue of 2.5.

In multiple-FEC configuration, two FEC OHs can be used. The requests R1, R2, and R3 are served with $QPSK_{20\%}$, as the SNRs with $QPSK_{20\%}$ are 6.0 dB, 4.78 dB, and 10.8 dB, respectively, according to (2), (4), (5), and (6), which are all over the threshold 4.58 dB. The AD node crosstalk in (2) and (7) is assumed to be zero for ease of calculation. Hence, for multiple-FEC configuration, the revenue is 3.7.

In the example, we see that the revenues can be improved by using multiple-FEC configuration. The traffic provisioning is composed by routing, MF, FEC, and spectrum assignment.

TABLE II
PARAMETERS AND VARIABLES IN RMAX

| | |
|---|---|
| **Network Sets and Parameters** | |
| $V, E$ | Node set and link set of the FON G. |
| $uv \in E$ | A link from node $u$ to $v$. |
| $s_i, d_i \in V$ | Source and destination node of request $i$. |
| $L_{uv}$ | Number of spans on link $uv$. |
| $F \in \mathbb{R}_{\geq 0}$ | Available spectrum resources of an optical fiber. |
| $N(v)$ | Adjacent node set of $v$ in G. |
| $D$ | Traffic demand list. |
| $i, j \in D$ | Any two requests $i$ and $j$ in traffic demand list $D$. |
| $r_i$ | Required bit-rate (Gbps) of request $i$. |
| $\eta_i$ | Revenue of request $i$. |
| $c \in \mathcal{C}$ | Transmission mode in candidate transmission mode set $\mathcal{C}$. |
| $\theta$ | A large constant. |
| $\epsilon_1$ | A factor balancing the importance between revenue and PLIs. |
| $o_q^1, o_q^0$ | Coefficients of piece-wise linear fitting function for fitting the XCI, $q \in \{1, 2, ..., Q\}$, where $Q$ is the number of segments. |
| **Variables in RMAX** | |
| $B_i \in \{0, 1\}$ | Equals 1 if request $i$ is accepted, 0 otherwise. |
| $q_v^i \in \{0, 1\}$ | Equals 1 if request $i$ goes into node $v$, 0 otherwise. |
| $p_v^i \in \{0, 1\}$ | Equals 1 if request $i$ goes out of node $v$, 0 otherwise. |
| $x_{uv}^i \in \{0, 1\}$ | Equals 1 if request $i$ uses link $uv$, 0 otherwise. |
| $x_{uv,c}^i \in \{0, 1\}$ | Equals 1 if request $i$ uses link $uv$ and transmission mode $c$, 0 otherwise. |
| $m_c^i \in \{0, 1\}$ | Equals 1 if request $i$ uses transmission mode $c$, 0 otherwise. |
| $f_i \in [0, F]$ | Center frequency of request $i$. |
| $f_{ij} \in [0, F]$ | Center frequency difference between requests $i$ and $j$. |
| $\Delta f_i \in [0, F]$ | Bandwidth of request $i$. |
| $\Delta f_{ij} \in [0, F]$ | Overlapping bandwidth between $i$ and $j$. |
| $f_{ij}^X \in [0, F]$ | Auxiliary variable of overlapping bandwidth $\Delta f_{ij}$. |
| $w_{ij} \in \{0, 1\}$ | Equals 1 if $f_i$ is greater than $f_j$, 0 otherwise. |
| $t_i^{\text{ASE}} \in \mathbb{R}_{\geq 0}$ | PLI of ASE noise of request $i$, $G_i^{\text{ASE}}/G_i$. |
| $t_i^{\text{SCI}} \in \mathbb{R}_{\geq 0}$ | PLI of SCI of request $i$, $G_i^{\text{SCI}}/G_i$. |
| $t_{ij,u}^{\text{XCI}} \in \mathbb{R}_{\geq 0}$ | Accumulated PLI of XCI of request $i$ from source node $s_i$ to $u$ that is generated by request $j$. |
| $t_{ij,v}^{\text{AD}} \in \mathbb{R}_{\geq 0}$ | Accumulated PLI of AD node crosstalk of request $i$ from source node $s_i$ to node $v$ that is generated by request $j$. |
| $h_c^{ij}$ | Piece-wise linear fitting term for XCI from $j$ to $i$ if $j$ takes transmission mode $c$. |
| $t_i^{\text{PLI}} \in \mathbb{R}_{\geq 0}$ | Total PLIs of request $i$. |

## IV. MILP FORMULATION

In this section, we formulate the revenue maximization problem as an MILP, named as RMAX. The parameters and variables of the MILP are summarized in Table II.

### A. MILP Model

To provision the lightpaths, both *network flow constraints* and *spectrum assignment constraints* must be taken into account. Besides, *SNR constraints* are also considered to ensure lightpaths' QoT. Thus, the problem is modeled as follows,

$$\max \quad \sum\nolimits_{i \in D} (\eta_i B_i - \epsilon_1 t_i^{\text{PLI}}) \quad \textbf{(RMAX)}$$
$$\textbf{\textit{s.t.}} \quad \text{Constraints} \quad (9) - (11)$$

The main objective of this MILP is to maximize the total revenue and the second objective is to minimize the total PLIs for all requests. The second objective, minimizing the total PLI of the requests, can reduce the PLIs and improve the SNR margin of network, which is regarded as an indirect way to balance the network performance [28]. The smaller the weighted factor $\epsilon_1$, the more emphasis on the revenue. For the sake of readability, we use $\forall i, \forall v, \forall uv, \forall c$ to denote $\forall i \in D, \forall v \in V, \forall uv \in E, \forall c \in \mathcal{C}$ in the following text.

*1) Network Flow Constraints:*

$$q_v^i = \sum_{u\in N(v)} x_{uv}^i \qquad \forall i,\forall v \qquad (9a)$$

$$p_v^i = \sum_{u\in N(v)} x_{vu}^i \qquad \forall i,\forall v \qquad (9b)$$

$$p_v^i - q_v^i = \begin{cases} B_i, & v = s_i \\ -B_i, & v = d_i \\ 0, & \text{others.} \end{cases} \qquad \forall i,\forall v \qquad (9c)$$

Constraints (9a) and (9b) determine the incoming and outgoing flow of request $i$ at node $v$. For any request $i$, the incoming degree $q_v^i$ counts 1 if request $i$ passes through or drops at node $v$. Also, for any request $i$, the outgoing degree $p_v^i$ counts 1 if request $i$ is added at or passes through node $v$. We will see that, with the help of $q_v^i$ and $p_v^i$, we can calculate the node crosstalk and other PLIs node-by-node. Constraints (9c) are the flow conservation constraints. If a request $i$ gets accepted ($B_i$=1), there exists a lightpath from the source node $s_i$ to the destination node $d_i$.

*2) Spectrum Assignment Constraints:*

$$\sum_{c\in\mathcal{C}} m_c^i = B_i \qquad \forall i \qquad (10a)$$

$$\Delta f_i \geq \sum_{c\in\mathcal{C}} \frac{r_i}{\mathrm{SE}(c)} m_c^i \qquad \forall i \qquad (10b)$$

$$w_{ij} + w_{ji} = 1 \qquad \forall i<j \qquad (10c)$$

$$\left.\begin{aligned} &f_i + \Delta f_i/2 \leq F \\ &0 \leq f_i - \Delta f_i/2 \end{aligned}\right\} \qquad \forall i \qquad (10d)$$

$$\left.\begin{aligned} &f_{ij} \leq f_i - f_j + 2F(1-w_{ij}) \\ &f_i - f_j \leq f_{ij} \end{aligned}\right\} \qquad \forall i<j \qquad (10e)$$

$$\Delta f_{ij} \geq \min\left(\Delta f_i, \Delta f_j, f_{ij}^X\right) \qquad \forall i<j \qquad (10f)$$

$$\Delta f_{ij} \leq F(2 - x_{uv}^i - x_{uv}^j) \qquad \forall uv,\forall i<j \qquad (10g)$$

$$\left.\begin{aligned} &\Delta f_{ij} = \Delta f_{ji} \\ &f_{ij} = f_{ji} \end{aligned}\right\} \qquad \forall i<j \qquad (10h)$$

Constraints (10a) select one transmission mode for non-blocked request $i$. Constraints (10b) define the bandwidth of request $i$ by its bit-rate and the adopted transmission mode. Constraints (10c) assure that either $w_{ij}$ or $w_{ji}$ should be equal to 1. Constraints (10d) limit the fiber spectrum within $[0, F]$. Constraints (10e) calculate the frequency difference $f_{ij}$ between $i$ and $j$. Constraints (10f) calculate the overlapping bandwidth $\Delta f_{ij}$. As it is not linear, we replace it with the following equations,

$$\begin{aligned} &\Delta f_{ij} \geq \min\left(\Delta f_i, \Delta f_j, f_{ij}^X\right) \\ &\Leftarrow \begin{cases} \Delta f_i - F a_{ij}^1 \leq \Delta f_{ij} \\ \Delta f_j - F a_{ij}^2 \leq \Delta f_{ij} \\ f_{ij}^X - F a_{ij}^3 \leq \Delta f_{ij} \\ 0 \leq f_{ij}^X \\ \dfrac{\Delta f_i + \Delta f_j}{2} - f_{ij} \leq f_{ij}^X \\ f_{ij}^X = f_{ji}^X \\ a_{ij}^1 + a_{ij}^2 + a_{ij}^3 = 2 \\ a_{ij}^1, a_{ij}^2, a_{ij}^3 \in \{0,1\} \end{cases} \qquad \forall i<j \end{aligned}$$

Constraints (10g) are spectrum non-overlapping constraints, indicating that when $i$ and $j$ share a common link, the overlapping bandwidth $\Delta f_{ij}$ on that link must be 0. Constraints (10h) guarantee that both variables $\Delta f_{ij}$ and $f_{ij}$ are symmetric.

*3) SNR Constraints:*

$$t_i^{\mathrm{ASE}} = \sum_{uv} \frac{G_i^{\mathrm{ASE}}}{G_i} L_{uv} x_{uv}^i \qquad \forall i \qquad (11a)$$

$$t_i^{\mathrm{SCI}} = \sum_{uv}\sum_{c} \mu G_i^2 L_{uv} \mathrm{asinh}\left(\rho\left(\frac{r_i}{\mathrm{SE}(c)}\right)^2\right) x_{uv,c}^i \qquad \forall i \qquad (11b)$$

$$x_{uv,c}^i + 1 \geq x_{uv}^i + m_c^i \qquad \forall i,\forall c,\forall uv \qquad (11c)$$

$$t_{ij,v}^{\mathrm{XCI}} - t_{ij,u}^{\mathrm{XCI}} + \theta(2 - x_{uv}^i - x_{uv,c}^j) \geq \mu G_j^2 h_c^{ij} L_{uv} \qquad \forall uv,\forall i\neq j,\forall c \qquad (11d)$$

$$t_{ij,v}^{\mathrm{XCI}} - t_{ij,u}^{\mathrm{XCI}} + \theta(1 - x_{uv}^i) \geq 0 \qquad \forall uv,\forall i\neq j \qquad (11e)$$

$$t_{ij,v}^{\mathrm{AD}} + \theta(3 - p_v^i - q_v^j - m_c^i) \geq \epsilon_{\mathrm{X}}(\Delta f_{ij} G_j)/(r_i/\mathrm{SE}(c) G_i) \qquad \forall c,\forall i\neq j,\forall v \qquad (11f)$$

$$t_i^{\mathrm{PLI}} \geq t_i^{\mathrm{ASE}} + t_i^{\mathrm{SCI}} + \sum_{j\neq i} t_{ij,d_i}^{\mathrm{XCI}} + \sum_{v}\sum_{j\neq i} t_{ij,v}^{\mathrm{AD}} \qquad \forall i \qquad (11g)$$

$$t_i^{\mathrm{PLI}} \leq \sum_{c\in\mathcal{C}} \frac{m_c^i}{\mathrm{SNR}_c^{\mathrm{th}}}, \qquad \forall i. \qquad (11h)$$

Constraints (11a) calculate PLI of ASE noise on the lightpath. Also, it is applied on the SCI calculation in constraints (11b). The variable $x_{uv,c}^i$, whether request $i$ uses link $uv$ and transmission mode $c$, is assured by the constraints (11c).

Since XCI is caused by two lightpaths, it will increase along their sharing links, and non-decrease along the other links. Constraints (11d) and (11e) implement the XCI calculation, respectively. But the nonlinear expression between XCI and $f_i$ makes a nonlinear calculation term $h_c^{ij}$. To address this issue, we replace the nonlinear term $h_c^{ij}$ by the following linear approximation $\hat{h}_c^{ij}$,

$$\begin{aligned} &h_c^{ij}\left(2\frac{|f_i - f_j|}{\Delta f_j}\right) \geq \ln\left(\frac{2|f_i - f_j|/\Delta f_j + 1}{2|f_i - f_j|/\Delta f_j - 1}\right) \qquad (12) \\ &\Leftarrow \hat{h}_c^{ij}(x) \geq \max\left(o_1^1 x + o_1^0, \cdots, o_q^1 x + o_q^0, \cdots, o_Q^1 x + o_Q^0\right) \\ &\Leftarrow \hat{h}_c^{ij} \geq o_q^1(2\mathrm{SE}(c) f_{ij}/r_j) + o_q^0 \qquad \forall i\neq j,\forall c, 1\leq q\leq Q \end{aligned}$$

where $o_q^1$ and $o_q^0$ are the coefficients of the $q^{\text{th}}$ segment of the piece-wise linear fitting. We use the least-square algorithm in [29] to fit the convex function $\ln\left(\frac{x+1}{x-1}\right)$ in the domain $x\in[x_1, x_2]$, where we set $x_1$=1.001, $x_2$=200, and $Q$=20. The fitting error $|\hat{h}_c^{ij} - h_c^{ij}|/h_c^{ij}$ can be minimized by increasing the number of segments $Q$. As shown in Fig. 4, the maximum fitting error is less than 5%.

Constraints (11f) calculate the node crosstalk along the lightpath, which is implemented by emphasizing the incoming degree $q_v^j$ of crosstalk signal $j$ and the outgoing degree $p_v^i$ of primary signal $i$. Constraints (11g) calculate the total PLIs of all traversed links and nodes. Constraints (11h) represent the QoT formulation.

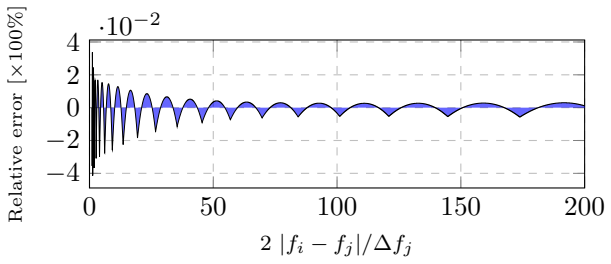


Fig. 4. Illustration for the fitting error performance of the piece-wise linear method. The fitting error is calculated by $(\hat{h}_c^{ij} - h_c^{ij})/h_c^{ij}$.

### B. Complexity Analysis

We analyze the number of constraints and variables in MILP model. The number of boolean variables $(q_v^i, p_v^i, x_{uv}^i, B_i, m_c^i, w_{ij}, a_{ij}^1, a_{ij}^2, a_{ij}^3, x_{uv,c}^i)$ is $|D|\{2|V| + (|E|+1)(|\mathcal{C}|+1)+4|D|-4\}$, and the number of real variables $(f_i, f_{ij}, f_{ij}^X, \Delta f_i, \Delta f_{ij}, t_i^{\text{ASE}}, t_i^{\text{SCI}}, t_{ij,v}^{\text{XCI}}, t_{ij,v}^{\text{AD}}, t_i^{\text{PLI}}, h_c^{ij})$ is $|D|\{5 + (|D| - 1)(3 + 2|V| + |\mathcal{C}|)\}$. The number of network flow constraints is $3|D||V|$, the number of spectrum assignment constraints is $|D|\{4+(|D|-1)(6+\frac{|E|}{2})\}$, and the number of SNR constraints is $|D|\{4 + |\mathcal{C}||E| + (|D| - 1)(|E| + \mathcal{C}(|E| + |V| + Q))\}$.

The MILP without PLI calculation is already NP hard and time-consuming [15]. Considering the scalability limitations, we also design a heuristic algorithm to solve the revenue maximization problem with lower complexity.

## V. Heuristic Algorithms

In this section, we design a decomposition algorithm, namely DEC-ALG, to solve (a) the problem of routing, and transmission mode assignment, *i.e.*, RTMA, and (b) the problem of spectrum assignment, *i.e.*, SA, separately. In RTMA, one assignment of the route and transmission mode pair is called as $\text{RTMA}_{\text{opt}}$, which has specified the route and transmission mode for all requests. The undetermined spectrum of the requests in $\text{RTMA}_{\text{opt}}$ will be assigned by the second subproblem. For comparison, we also present a heuristic as benchmark, which is adapted from existing literature.

While solving the first subproblem RTMA, we adopt an improved strategy that repeatedly generates multiple $\text{RTMA}_{\text{opt}}$ solutions and stores them in a solution pool. In the repetition process, two methods are used to guarantee a new $\text{RTMA}_{\text{opt}}$ solution, method 1 excluding previous $\text{RTMA}_{\text{opt}}$ and method 2 perturbing the transmission mode set. After receiving the respective $\text{RTMA}_{\text{opt}}$ solution in the solution pool, the second subproblem SA assigns the spectrum for each request by scanning the available spectrum resources on the assigned route, where three constraints have to be satisfied (*i.e.*, spectrum contiguity, spectrum continuity, and SNR constraints). Finally, we calculate the revenue of the requests successfully assigned by SA and take the maximum revenue of the multiple $\text{RTMA}_{\text{opt}}$ solutions as the final result.

### A. DEC-ALG

Before running the DEC-ALG, we precalculate several parameters for each request including the values of ASE, SCI, and residual margin for different routes and transmission modes. Candidate routes are obtained by the $K$ shortest path algorithm [30], while transmission modes are taken from the $\mathcal{C}$. For any request $i$, the tuple $(\xi_i, c_i)$ denotes such route and transmission mode pair. The ASE and SCI are known impairments for a given $(\xi_i, c_i)$, which are obtained by (4) and (5). Unlike the ASE and SCI, the node crosstalk and XCI cannot be known a-prior, because they require the knowledge of the exact spectrum allocation of other lightpaths. Hence, we estimate the quality of each lightpath by using the residual margin $\phi_{i\xi c}$, which is expressed as follows,

$$\phi_{i\xi c} = \frac{\phi}{\text{SNR}_c^{\text{th}}} - t_i^{\text{ASE}} - t_i^{\text{SCI}} - \epsilon_{\text{X}} \sum_{v \in V_{i\xi}} \frac{N(v)+1}{2} \tag{13}$$

where $\phi$ is an estimated ratio considering the ASE and SCI. Other related parameters and variables in DEC-ALG are explained in Table III. In (13), the known impairments of ASE and SCI are fully considered, while the unknown impairments of AD node crosstalk are only estimated with an average.

TABLE III
Parameters & Variables in Algorithm DEC-ALG

| | |
|---|---|
| **Network sets & Parameters** | |
| $\phi \in [0,1]$ | A ratio on SNR threshold considering ASE+SCI. $1-\phi$ represents the part considering XCI+AD. $\phi = 0.9$ is considered in this paper. |
| $P_i$ | Route and transmission mode pairs set $(\xi, c)$ of request $i$. |
| $P_{ie}$ | Route and transmission mode pairs set $(\xi, c)$ of request $i$ that traverses link $e$. |
| $V_{i\xi}$ | Node set on the $\xi$-th route of request $i$. |
| $\epsilon_2$ | Factors balancing the weight of SNR margin and revenue. |
| $b_i, e_i$ | Spectrum beginning and end of request $i$. |
| $\phi_{i\xi c} \in \mathbb{R}$ | Estimated SNR margin of request $i$ using transmission mode $c$ and $\xi$-th route after RTMA. |
| $\Delta f_{ic}$ | Bandwidth of request $i$ using transmission mode $c$. |
| $N_{\text{RTMA}}$ | Number of $\text{RTMA}_{\text{opt}}$ solutions. |
| $N_{\text{round}}$ | Number of attempts in the spectrum assignment. |
| **Variables** | |
| $B_i \in \{0,1\}$ | Equals 1 if request $i$ is accepted, 0 otherwise. |
| $g_{i\xi c} \in \{0,1\}$ | Equals 1 if request $i$ uses the $\xi$-th route and transmission mode $c$, 0 otherwise. |
| $\phi_{\text{avg}}$ | Average SNR margin of all requests. |

*1) RTMA:* Using the precalculated parameters, this model selects one route and transmission mode pair, based on the following RTMA model,

$$\max \quad \sum_{i \in D} \eta_i B_i + \epsilon_2 \phi_{\text{avg}} \quad \textbf{(RTMA)}$$

$$\textbf{\textit{s.t.}} \sum_{(\xi,c) \in P_i} g_{i\xi c} = B_i \qquad \forall i \tag{14a}$$

$$\sum_{i \in D} \sum_{(\xi,c) \in P_{ie}} \Delta f_{ic} g_{i\xi c} \le F \qquad \forall e \tag{14b}$$

$$0 \le \sum_{(\xi,c) \in P_i} g_{i\xi c} \phi_{i\xi c} \qquad \forall i \tag{14c}$$

$$\phi_{\text{avg}} = \frac{1}{|D|} \sum_{i \in D} \sum_{(\xi,c) \in P_i} g_{i\xi c} \phi_{i\xi c}. \tag{14d}$$

The main objective of RTMA is to maximize the accepted revenue and the second one is to maximize average SNR

margin. In the multi-objective function, the importance of the revenue can be lowered by increasing the weight factor $\epsilon_2$. Constraints (14a) make sure that a route and transmission mode pair $(\xi, c)$ is assigned for request $i$ if $B_i$=1. Constraints (14b) restrict the spectrum usage of each link. Bandwidth requirement of $i$ with the transmission mode $c$, denoted by $\Delta f_{ic}$, equals $r_i/\text{SE}(c)$. Constraints (14c) make sure that the minimum SNR margin is non-negative. Constraint (14d) defines the average SNR margin of all requests.

In RTMA, only one $\text{RTMA}_{\text{opt}}$ solution is obtained. However, this solution may not bring the maximum revenue after spectrum assignment. To this end, we intend to generate multiple $\text{RTMA}_{\text{opt}}$ solutions ($\times N_{\text{RTMA}}$), which is completed by the following two methods, **excluding the previous $\text{RTMA}_{\text{opt}}$ constraint** and **perturbing the transmission mode set**.

**Method 1 : excluding the previous $\text{RTMA}_{\text{opt}}$**. This method excludes the previous $\text{RTMA}_{\text{opt}}$ solution by adding constraints (15) to RTMA, where both $B_i^{<n-1>}$ and $g_{i\xi c}^{<n-1>}$ are the results from the $(n-1)^{\text{th}}$ solution.

$$\sum_{\substack{i\in D\\ B_i^{<n-1>}=1}} \sum_{\substack{(\xi,c)\in P_i\\ g_{i\xi c}^{<n-1>}=1}} g_{i\xi c} + \frac{1}{K|\mathcal{C}|} \sum_{\substack{i\in D\\ B_i^{<n-1>}=0}} \sum_{\substack{(\xi,c)\in P_i\\ g_{i\xi c}^{<n-1>}=0}} (1-g_{i\xi c}) \leq |D| - \frac{1}{K|\mathcal{C}|}, n \in \{1,2,3,\cdots,N_{\text{RTMA}}\} \tag{15}$$

In the following, we provide more explanations for the excluding constraints (15).

In the $n^{\text{th}}$ loop, we suppose a contrary case that generates the identical $\text{RTMA}_{\text{opt}}$ to the previous solutions, *i.e.*, $\forall i, (\xi, c)$, the variables $g_{i\xi c}$ all equal $g_{i\xi c}^{<n-1>}$. Then, the value of the left side in constraints (15) becomes $|D|$, which is greater than the right side $|D| - \frac{1}{K|\mathcal{C}|}$. Therefore, we can say that the contrary case is false and constraints (15) hold *only if* $\exists i, (\xi, c), g_{i\xi c} \neq g_{i\xi c}^{<n-1>}$, or equivalently, constraints (15) are sufficient for generating a different $\text{RTMA}_{\text{opt}}$ solution.

Next, we discuss whether constraints (15) are necessary for generating a different $\text{RTMA}_{\text{opt}}$ solution. Let us focus on a request $\imath$ that satisfies $g_{\imath\xi c} \neq g_{\imath\xi c}^{<n-1>}$, which denotes a different $\text{RTMA}_{\text{opt}}$ solution. We use $(\bar{\xi}, \bar{c})$ to denote the index of tuples for that request using different route and transmission mode pairs. Thus, we can say $(g_{\imath\bar{\xi}\bar{c}}^{<n-1>}, g_{\imath\bar{\xi}\bar{c}}) = (1, 0)$ or $(0, 1)$. Since constraints (14a) require the request $\imath$ should satisfy $\sum_{(\xi,c)} g_{\imath\xi c}^{<n-1>} = B_\imath^{<n-1>} \leq 1$, we discuss the two possible cases respectively, (I) $B_\imath^{<n-1>} = 1$ and (II) $B_\imath^{<n-1>} = 0$.

- (I) $B_\imath^{<n-1>} = \sum_{(\xi,c)} g_{\imath\xi c}^{<n-1>} = 1$ holds, thus $g_{\imath\bar{\xi}\bar{c}}^{<n-1>} = 1$, we can get

$$\left.\begin{aligned} &\sum_{(\xi,c)} g_{\imath\xi c}^{<n-1>} = 1\\ &\exists(\bar{\xi},\bar{c}), g_{\imath\bar{\xi}\bar{c}} \neq g_{\imath\bar{\xi}\bar{c}}^{<n-1>}\\ &\sum_{(\xi,c)} g_{\imath\xi c} \leq 1 \end{aligned}\right\} \Rightarrow \begin{cases} g_{\imath\bar{\xi}\bar{c}} = 0,\\ \sum\limits_{(\xi,c)=(\bar{\xi},\bar{c})} g_{\imath\xi c} = 0 \end{cases} \tag{16}$$

- (II) $B_\imath^{<n-1>} = \sum_{(\xi,c)} g_{\imath\xi c}^{<n-1>} = 0$ holds, then we can get the result $\frac{1}{K|\mathcal{C}|} \sum_{\substack{(\xi,c)\in P_i\\ g_{\imath\xi c}^{<n-1>}=0}} (1-g_{\imath\xi c}) = \frac{K|\mathcal{C}|-1}{K|\mathcal{C}|}$ with the following proof,

$$\left.\begin{aligned} &\sum_{(\xi,c)} g_{\imath\xi c}^{<n-1>} = 0\\ &\exists(\bar{\xi},\bar{c}), g_{\imath\bar{\xi}\bar{c}} \neq g_{\imath\bar{\xi}\bar{c}}^{<n-1>}\\ &\sum_{(\xi,c)} g_{\imath\xi c} \leq 1 \end{aligned}\right\} \Rightarrow \begin{cases} g_{\imath\bar{\xi}\bar{c}} = 1,\\ g_{\imath\xi c} = 0, (\xi,c) \in P_\imath \backslash \{\bar{\xi},\bar{c}\}\\ \sum\limits_{(\xi,c)\in P_i} (1-g_{\imath\xi c}) = K|\mathcal{C}| - 1 \end{cases} \tag{17}$$

We denote by $n_{(16)}$ and $n_{(17)}$ the number of requests satisfying (16) and (17), respectively. In addition, for the request $i$ that does not change the route and transmission mode, *i.e.*, $\forall(\xi, c), g_{i\xi c} = g_{i\xi c}^{<n-1>}$, the first item of left sides of constraints (15) equals 1. The number, denoted by $n_1$, must be less than $|D|-1$. Thus, we can get the sum of the left sides, $0 \cdot n_{(16)} + 1 \cdot n_1 + (1 - \frac{1}{K|\mathcal{C}|}) \cdot n_{(17)} \leq |D| - \frac{1}{K|\mathcal{C}|}$. We observe that the upper bound is $|D| - \frac{1}{K \cdot |\mathcal{C}|}$, which is precisely equal to the right side of the constraints (15). Thus, we can say that constraints (15) *hold if* there is a different $\text{RTMA}_{\text{opt}}$ solution.

**Method 2 : perturbing the transmission mode set**. This method forces the least number of each transmission mode in $\text{RTMA}_{\text{opt}}$. It is worth mentioning that the method 1 should be repeated with $(K|\mathcal{C}|+1)^{|D|}$ times to cover the solution space of $\text{RTMA}_{\text{opt}}$. However, with small $N_{\text{RTMA}}$, *i.e.*, $N_{\text{RTMA}} \ll (K \cdot |\mathcal{C}| + 1)^{|D|}$, the potential $\text{RTMA}_{\text{opt}}$ solution is insufficient to cover the solution space that includes the maximum revenue. Thus, it may happen that we obtain the same revenue from two different transmission mode configurations when we randomly choose the transmission mode.

To solve the mentioned issue caused by the random transmission mode selection strategy, we use a *perturbation method* that ensures the minimum utilization of a transmission mode $l$. The $\text{RTMA}_{\text{opt}}$ solution is extended by using its subset $\mathcal{C}_{sub}^{<l>}$. Each subset takes $l$ elements from $\mathcal{C}$. Briefly, for the $l^{\text{th}}$ subset $\mathcal{C}_{sub}^{<l>}$, the $l^{\text{th}}$ transmission mode of $\mathcal{C}$ is added compared to the previous $l-1$ subsets. Constraints (18) are used to generate $\text{RTMA}_{\text{opt}}$ using the subset $\mathcal{C}_{sub}^{<l>}$ that forces the use of a transmission mode $c^l$ but excludes the use of the other transmission modes $c^r$ that greater than $c^l$,

$$\sum_{i\in D, 1\leq\xi\leq K} g_{i\xi c^l} \geq 1, \qquad c^l \in |\mathcal{C}| \tag{18a}$$

$$\sum_{i\in D, 1\leq\xi\leq K} g_{i\xi c^r} = 0, \qquad \forall c^r \in \mathcal{C}\backslash\mathcal{C}_{sub}^{<l>} \tag{18b}$$

With the above RTMA model and solution pool strategy, we can gather at most $N_{\text{RTMA}}|\mathcal{C}|$ solutions and guarantee that each transmission mode is utilized. We use the pseudo-code in Algorithm 1 to illustrate the procedure. In line 4, the model is initialized with the constraints (14) and the input parameters $\text{G}(V, E)$, $D$, $N_{\text{RTMA}}$, and $\mathcal{C}$. In line 6, $\text{RTMA}_{\text{opt}}$ solution with $g_{i\xi c} = 0$ is initialized. Then, from lines 7 to 10, the RTMA model is repeated using method 1.

**Algorithm 1:** Generating multiple $\text{RTMA}_{\text{opt}}$ schemes

**Input :** $\text{G(V, E)}, D, N_{\text{RTMA}}, \mathcal{C}$
**Output:** $\boldsymbol{g}$
1 **for** $\mathcal{C}_{sub}^{<l>} \subset \mathcal{C}$ **do**
2 // Method 2
3 Initialize the current transmission mode set $\mathcal{C}_{sub}^{<l>}$ that emphasizes the transmission mode $c^l$;
4 Create the RTMA model with the constraints in (14) and with the input parameters of G(V,E), $D$, $N_{\text{RTMA}}$, and $\mathcal{C}_{sub}^{<l>}$;
5 Update the RTMA model with the constraints (18);
6 $g_{i\xi c}^{<0>} \leftarrow 0, \forall i, (\xi, c)$ // $g_{i\xi c}^{<0>} \in \boldsymbol{g^{<0>}}$
7 **for** $n \in \{1, 2, ..., N_{RTMA}\}$ **do**
8 // Method 1
9 Update RTMA model using excluding constraints (15) and the previous solutions;
10 Solve RTMA model and save the $\text{RTMA}_{\text{opt}}$ solution as $\boldsymbol{g^{<n>}}$;

*2) SA:* Once the RTMA problem is solved, from the solution $\text{RTMA}_{\text{opt}}$, we can obtain the pair index of route and transmission mode of each request $i$. Then, with the assigned route and transmission mode in $\text{RTMA}_{\text{opt}}$ $(\bar{\xi}_i, \bar{c}_i) = \{(\xi, c)|g_{i\xi c} = 1, i \in D\}$, we allocated an exact spectrum position for each request by first-fit strategy and by sequentially scanning the available spectrum resources, where both (*i*) spectrum continuity and (*ii*) spectrum contiguity constraints are considered.

The third constraint, (*iii*) SNR constraint, should also be taken into account when scanning spectrum resources. Due to the unknown fiber nonlinear interference and AD node crosstalk, the SNR of both the new request and existing requests may degrade once the new request is allocated, thus the new request can be assigned successfully only if the following two conditions hold, (*i*) the current request has a satisfactory QoT; (*ii*) existing requests also have a satisfactory QoT. If either one is unsatisfied, the spectrum interval of the new request is moved until a feasible interval is found or fiber spectrum is fully explored.

Also, due to the nonlinear interference and node crosstalk, a problematic dead-lock case may happen as the requests accumulate in the network. For example, if some requests with very little SNR margin are allocated, this might result in high probability of rejecting the future lightpath sharing the common nodes or links. So, to ensure the blocked requests can be accepted again, we repeat the assignment process $N_{\text{round}}$ times. For the request in each round, the *required margin* between SNR and SNR threshold is designed to decrease gradually, and equals zero in the final round.

The SA procedure is illustrated in Algorithm 2. In line 1, we sort the requests by function ARRANGE, which will be explained later. In line 4, we set the minimum *required margin* for each request with the value $\frac{N_{\text{round}} - n_{\text{round}}}{N_{\text{round}}}$. Then, in lines 6 and 7, the required spectrum bandwidth and route are extracted from the $\text{RTMA}_{\text{opt}}$ solution. In line 8, we merge the available

**Algorithm 2:** Spectrum Assignment

**Input :** $\boldsymbol{g}$
**Output:** $\boldsymbol{alloc}$
1 $D_{\text{arr}} \leftarrow$ **ARRANGE**$(D)$;
2 $\boldsymbol{alloc} \leftarrow \mathbf{0}$ // $alloc_i \in \boldsymbol{alloc}$;
3 **for** $n_{round} \in [1, ..., N_{round}]$ **do**
4 Skip the request $i$ if it cannot satisfy the minimum SNR margin in the current $n_{\text{round}}^{\text{th}}$ round;
5 **for** $i \in D_{arr}$ & $!alloc_i$ **do**
6 $(\bar{\xi}_i, \bar{c}_i) \leftarrow \{(\xi, c)|g_{i\xi c} = 1\}$// $g_{i\xi c} \in \boldsymbol{g}$;
7 $\Delta f_i \leftarrow r_i/\text{SE}(\bar{c}_i)$ ;
8 $\text{MERGED}_{\text{space}} \leftarrow$ available spectrum space on $\bar{\xi}_i^{\text{th}}$ route;
9 Find an initial offset $b_i^{\Delta}$ based on the $\text{MERGED}_{\text{space}}$;
10 **for** *the spectrum beginning* $b_i$*:* $b_i^{\Delta} \rightarrow F - \Delta f_i$ *with step* $\Delta$*=12.5 GHz &* $!alloc_i$ **do**
11 **if** $[b_i, b_i + \Delta f_i] \in \text{MERGED}_{\text{space}}$ **then**
12 **try :**
13 Assign $[b_i, b_i + \Delta f_i]$ on $\bar{\xi}_i^{\text{th}}$ route;
14 Check QoT of assigned requests by (3);
15 Check QoT of current request $i$ by (3);
16 $alloc_i \leftarrow 1$;
17 **catch** *Check failed***:**
18 $alloc_i \leftarrow 0$;

spectrum of the $\xi^{\text{th}}$ route and assign it to $MERGED_{\text{space}}$, where both spectrum continuity and spectrum contiguity constraint are satisfied. Then, from lines 10 to 18, the algorithm SA tries to search a spectrum interval $[b_i, b_i + \Delta f_i]$ from $MERGED_{\text{space}}$ that satisfies the QoT. An increment of 12.5 GHz has been used when scanning the spectrum, which aims at lowering the complexity of searching the available spectrum resources while reducing the unexpected XCI and AD node crosstalk. An improved strategy that sequentially assigns and optimizes the spectrum can refer to our another optimization [21].

In the ARRANGE function of Algorithm 2, we sort the requests by four different assignment policies, *random order* $\Delta f_i$ (SA), descending order of *bandwidth* $\Delta f_i$ (SA-B), *revenue* $\eta_i$ (SA-R), and *revenue to bandwidth ratio* $\eta_i/\Delta f_i$ (SA-RA), respectively. The performances of these four arrangement policies are compared in simulations.

### *B. Complexity Analysis of DEC-ALG*

In the first subproblem RTMA, the number of variables $(g_{i\xi c}, B_i)$ is $|D|(K|\mathcal{C}| + 1)$, and the number of constraints is $2|D| + |E| + 1$. Using the pool strategy, the number of additional constraints is $N_{\text{RTMA}} \frac{N_{\text{RTMA}} - 1}{2} + |\mathcal{C}|$ but no additional variable is required.

For the spectrum assignment SA, the complexity depends on two modules, the spectrum scanning process and the spectrum

merging function. The former could be $\mathcal{O}(\frac{F}{12.5})$ in the worst-case. The latter is $\mathcal{O}(k_A + k_B)$, where $k_A$ and $k_B$ are the number of isolated spectrum intervals in the two spectrum spaces to be merged, $A$ and $B$ [31].

### C. Benchmark Algorithm

To efficiently utilize the spectrum resource of fiber, a large number of algorithms on traffic provisioning have been proposed. To make a fair comparison, we take the algorithm in [25] that also adopts the continuous spectrum allocation. The benchmark algorithm, called as REF-A in this paper, is implemented by three steps, (*i*) RTMA model with limited spectrum resources and with the objective of maximizing the revenue, (*ii*) allocating the channel ordering for each request, and (*iii*) allocating the exact spectrum for each request. It should also be noted that the spectrum assignment of REF-A, (*ii*) and (*iii*), is implemented by two complex LP models rather than the one-step heuristic algorithm in our paper. In addition, its PSD is assumed to be a constant, as in this paper.

## VI. Illustrative Numerical Results

In this section, we present the numerical experiment results. First, we compare the efficiency of our proposed heuristic and the MILP model. Then, we investigate revenues in scenarios with different PSDs and different transmission modes. Finally, we consider the experiments for severe resource crunch scenarios, which is simulated by increasing bit-rate and number of requests.

The MILP, heuristic algorithm DEC-ALG, and REF-A run on an Intel Core PC with 4.0 GHz CPU and 16 GB RAM. Specifically, we solved the MILP model by CPLEX 12.6 and implemented the two heuristic algorithms using an ad-hoc code developed in C++. Maximum computing time for the MILP was fixed to one hour. All illustration results have been averaged over 10 independent simulation runs to guarantee statistical accuracy.

The 6-node network in Fig. 3, German(9 nodes, 34 links), NSFNET(14 nodes, 44 links), US Backbone(28 nodes, 90 links) networks in [21, 32] are used as case study topologies. Note that, since only a small number of path length of NSF network and US Backbone network can support high-order MF, we divide the length of link by 6 in the simulations. The spectrum resource of each fiber $F$ is assumed with 1,000 GHz to increase the simulation speed for large networks. The algorithm parameter $\epsilon_1$=0.01 and $\epsilon_2$=0.001 are adjusted to be small to emphasize the revenue rather than the other parameters for simulation. The parameters $N_{\text{RTMA}}$=40, $N_{\text{round}}$=2, and $K$=4 are adjusted to guarantee stable simulation results in a reasonable time. The bit-rates $r_i$ are randomly chosen from the set {250, 500, ..., 250+$n$*250, ... 250+2$n$*250} Gbps. For the lowest bit-rate, the channel can be guaranteed with bandwidth over than 28 GHz with PM-16QAM [25], which is acceptable for the GN model calculation in [18]. The large bit-rate request is assumed by super-channel with large baud rates. The initial launch power PSD is simplified with a local optimal value of $-16$ dBm/GHz by using the LOGON strategy [33] for one

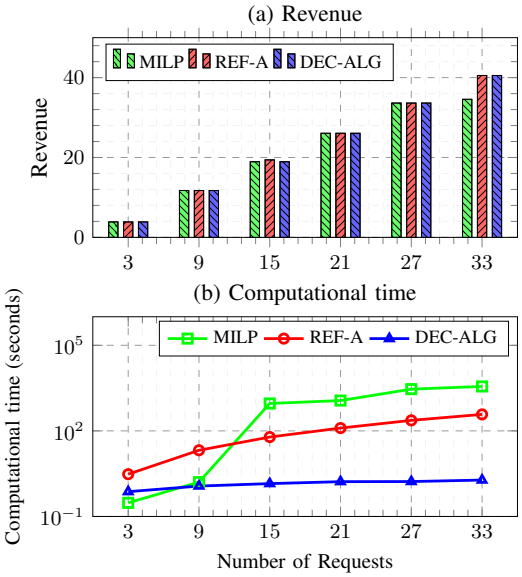


Fig. 5. Comparison of revenue and computational time in 6-node network.

span with the heaviest spectral loads. The definition of revenue and other used notations for simulation are given as follows,

1) *Revenue*: $\eta_i = u_i$, where $u_i$ is the service type parameter. This paper considers the service type parameter $u_i$ follows the Zipf distribution Zipf(1,5) [34]. The revenue of a network is sum of all accepted lightpaths' revenue.
2) *Adaptive MFs* : $\mathcal{C} = (\hat{\mathcal{M}}_m, \mathcal{F}_f)$. Notation $\mathcal{F}_f$ represents the $f^{\text{th}}$ level FEC, and $\hat{\mathcal{M}}_m$ represents all the MFs not beyond the $m^{\text{th}}$ order. FEC OH of 7% is used by default if we do not mention the FEC.
3) *Multiple FECs*: $\mathcal{C} = (\mathcal{M}_m, \hat{\mathcal{F}}_f)$. Notation $\mathcal{M}_m$ represents the $m^{\text{th}}$ order MF, and $\hat{\mathcal{F}}_f$ represents the FEC OHs not beyond the $f^{\text{th}}$ one. QPSK is used by default if we do not mention the MF.

### A. Validation Using MILP

We validate the MILP on the 6-node network. The bit-rate per request is fixed at 1,000 Gbps. Figure 5 illustrates the revenue and computational time of three algorithms as the number of requests increases.

In Fig. 5, we can observe that the computational time of MILP reaches the preset maximum computing time one hour, when the number of requests increases to 33. It means that MILP is intractable, even in the case with either small networks or small number of requests. But the heuristic algorithm REF-A and DEC-ALG can solve it in a few minutes and a few seconds, respectively. Besides, we observe that both DEC-ALG and REF-A are able to obtain an approximate optimal value of MILP. Therefore, the proposed algorithm DEC-ALG is not only time-efficient but also near-optimal.

In the ARRANGE function of SA of the DEC-ALG algorithm, we have mentioned four different sorting policies for requests. In order to find the best sorting policy, we compared their results in Fig. 6. The simulation is carried out in NSF network. As we see in Fig. 6, the revenue with different sorting

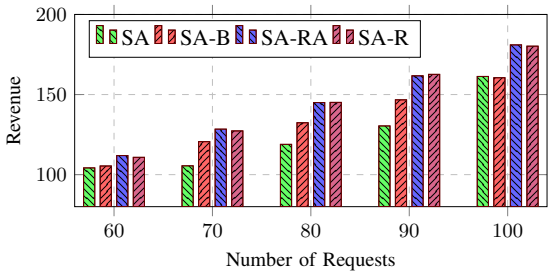


Fig. 6. Revenue comparison with four different sorting policies of ARRANGE function.

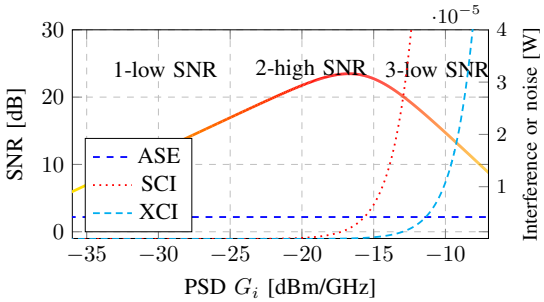


Fig. 7. SNR vs. PSD $G_i$.

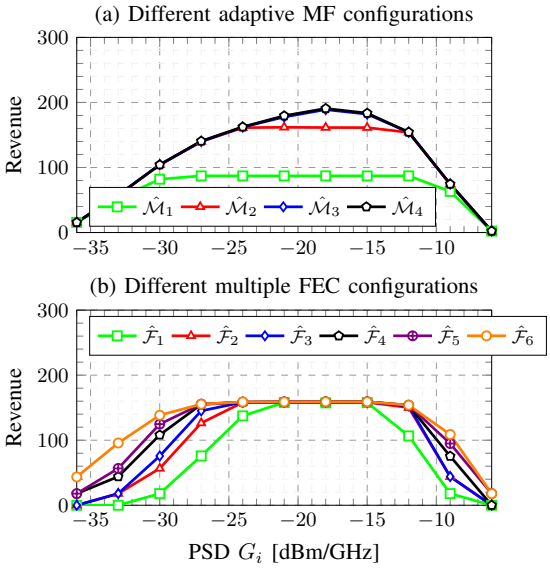


Fig. 8. Impact of PSD.

policies increases with the number of requests. It can also be seen that SA-RA, which sorts the requests by the descending order of revenue/bandwidth ratio, gets the largest revenue. Therefore, we confirm to use SA-RA for heuristic algorithm DEC-ALG.

### *B. Impacts of PSD, MF and FEC*

As we have seen in the example of Fig. 3, revenues can be influenced by SNR requirements of different transmission mode configurations. In (4), (5), and (6), when PSD $G_i$ increases, the ASE noise keeps the same, while the interference SCI and XCI will increase cubically. The PSD of ASE noise, SCI, and XCI, as well as the SNR for an example request of 250 Gbps and with PM-QPSK$_{7\%}$ in the middle of a fully occupied fiber span are illustrated in Fig. 7. According to the SNR and PSD, we briefly distinguish three different scenarios, namely scenario 1: *low SNR with low PSD*, scenario 2: *high SNR with median PSD*, and scenario 3: *low SNR with high PSD*. By adjusting PSDs, we can investigate the revenue impact of MF and FEC in different SNR scenarios.

First, we fix FEC OH at 7% and compare different MFs as PSD varies. The simulation results of NSF network using 100 requests and 1,000 Gbps per request are illustrated in Fig. 8(a). It is observed that the revenue of different MFs increases as PSD changes from scenario 1 to 2, but then decreases from scenario 2 to 3. Both adaptive MF $\hat{\mathcal{M}}_3$ and $\hat{\mathcal{M}}_4$ that contain MFs {BPSK, QPSK, 8QAM} get the largest revenue in scenario 2, with 118% improvement compared to $\hat{\mathcal{M}}_1$. It can be explained by the SNR threshold and spectral efficiency of different MFs. Only in the scenario with high SNR, high-order MFs can be adopted, which reduces the spectrum usage and spares more spectrum resources for other requests. However, in the scenario with low SNR, the adaptive method with four MFs has no difference with either one MF or two MFs, because the high-order MF cannot be adopted.

Then, we fix MF at QPSK and compare multiple FECs. The results are illustrated in Fig. 8(b), where we can see that, also in this case, as PSD changes from scenario 1 to 2, the revenue of different FEC increases, while from scenario 2 to 3, the revenue decreases. Different from the adaptive MF, having multiple FEC choices has a tiny impact on revenue difference on scenario 2, while a greater difference is only observed for both scenarios 1 and 3, which is a different result with respect to adaptive MF. In low SNR scenario, most lightpaths with small FEC OHs are blocked, while the redundant FEC with large FEC OHs can lower the SNR requirement and provide more SNR margins to overcome the PLIs. This is the reason for high revenue in low SNR scenario. But in the high SNR scenario, the redundant FEC loses such advantage because many requests have adopted the only transmission mode $f_1$ with the highest spectral efficiency. Therefore, no revenue improvement can be observed in this scenario.

Given the suitable PSD scenario of multiple FECs and adaptive MF, we further investigate the impact of joint MF and FEC schemes in NSF, US Backbone, and German network. The revenues of 100 requests with average bit-rate 1,000 Gbps are illustrated in Fig. 9. In Fig. 9(a) with high SNR and median PSD ($G_i = -18$ dBm/GHz), we find that the adaptive MFs enable to improve the revenue, while the configuration of multiple FECs has a weak impact on the revenue. In Fig. 9(b) with low SNR and with high PSD ($G_i = -9$ dBm/GHz), both adaptive MFs and multiple FECs enable to improve the revenue, which means that the combination of MF and FEC is preferred in high PSD scenario rather than median PSD scenario. We also find that the revenue of adaptive MF configuration $\hat{\mathcal{M}}_3$ and multiple FEC configuration $\hat{\mathcal{F}}_5$ can reach the almost maximum value for both high and low SNR scenarios. It means that the usage of MF with PM-16QAM

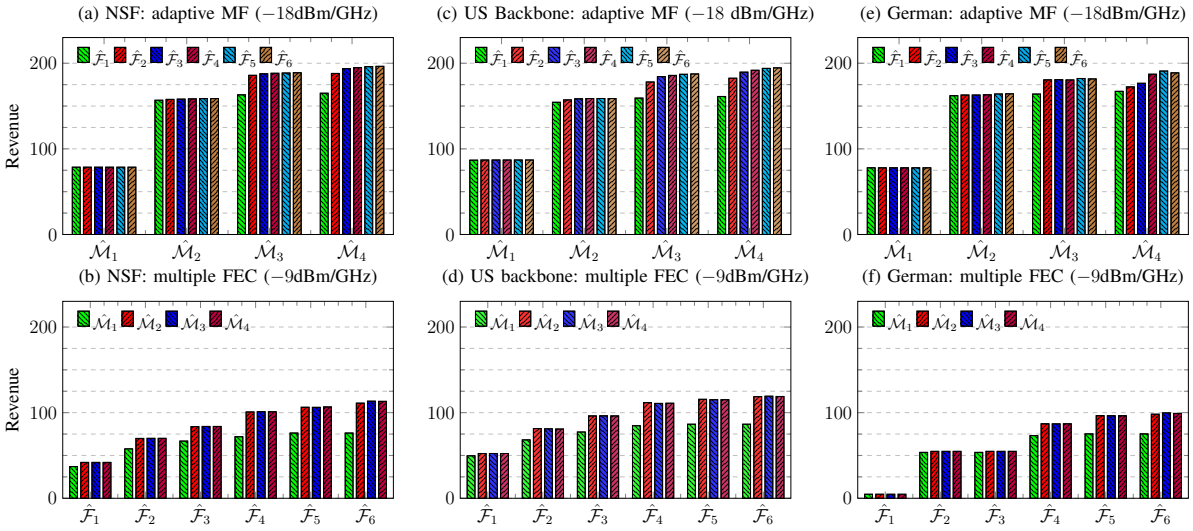


Fig. 9. Revenue impact of joint MF and FEC for NSF network, (a) and (b); US Backbone network, (c) and (d); German network, (e) and (f).

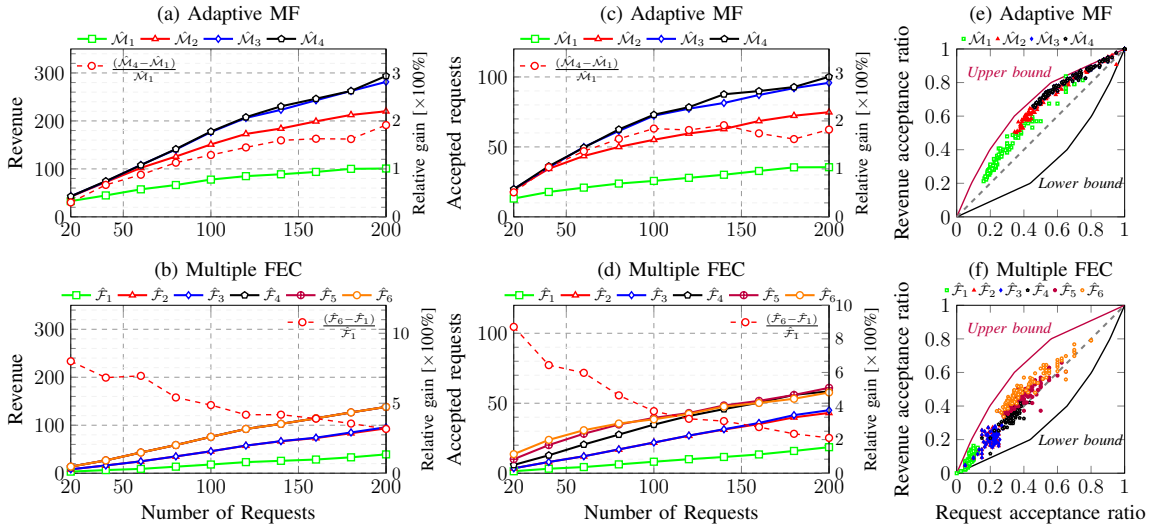


Fig. 10. Impact of accepted revenue and accepted requests of adaptive MF and multiple FEC in NSF network. Bit rate per request is 1,000 Gbps.

and FEC OH with 50% can be saved. Similar results can also be observed in US Backbone network and German network.

### C. Different Traffic Loads

Two metrics, accepted revenue and number of accepted requests, will be analyzed in static networks, where we assume different average bit-rates and the different number of requests. Besides, we also report the results in dynamic traffic loads.

*1) Static Network:* Let us now study the impact of different numbers of requests. The simulations assume all requests with identical 1,000 Gbps. The PSD is either -18 dBm/GHz or -9 dBm/GHz, such that we operate in scenarios that benefit of adaptive MFs and multiple FECs, respectively. The results of different adaptive MFs and different FECs are shown in Fig. 10. In Fig. 10(a), the four adaptive MFs obtain the same result with 20 requests, but, as the number of requests increases, the relative gain achieved by using four different adaptive MFs also increases. The maximum improvement of adaptive MFs (192% higher compared to $\hat{\mathcal{M}}_1$) is obtained with 200 requests. In Fig. 10(b), multiple FECs' revenue also increases with the number of requests. Configuration $\hat{\mathcal{F}}_6$ gets the largest revenue, which is 3.2 times higher than $\hat{\mathcal{F}}_1$.

As all the results are based on the assumption that the service type parameter follows the Zipf distribution, the results on the number of accepted requests could help demonstrate to which degree the revenue depends on the assumption. Thus, we show the accepted requests and revenue in Figs. 10(c) and (d). We also show the acceptance ratio of revenue and requests in Figs. 10(e) and (f), where the revenue acceptance ratio is defined as $\frac{\sum_i \eta_i B_i}{\sum_i \eta_i}$ and the request acceptance ratio is defined as $\frac{\sum_i B_i}{|D|}$. The positive correlation relationship between the two ratios reveals that maximizing revenues also guarantees a higher request acceptance ratio. Besides, the revenue acceptance ratio is greater than the request acceptance ratio (above the curve $y = x$ in gray dashed line), which shows a greater advantage and efficiency of our algorithm in

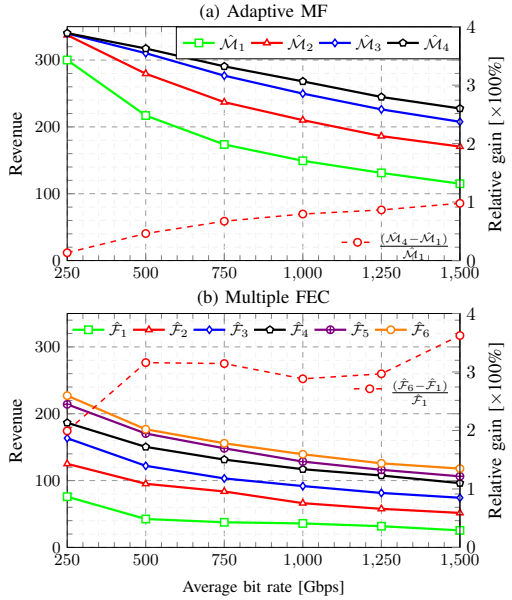


Fig. 11. Revenue impact with different traffic rates in NSF network. The simulations use 160 requests.

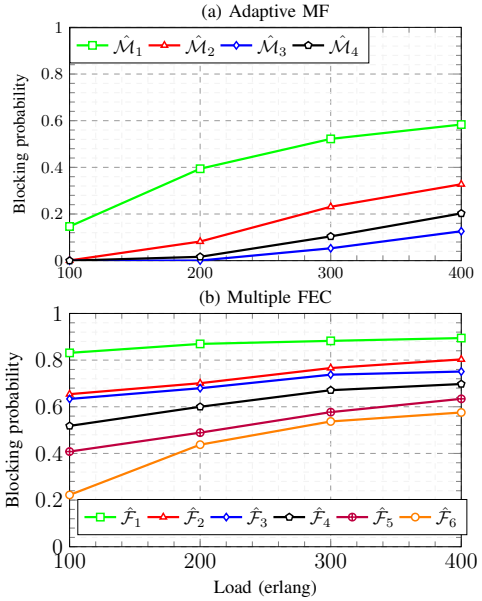


Fig. 12. Comparison for adaptive MF and multiple FEC in dynamic traffic in NSF network assumed with -18 dBm/GHz for (a) and -9 dBm/GHz for (b).

collecting revenues.

We report the simulation results with different average bit-rates in Fig. 11. For a given average bit rate of 250+$n$*250, each request can randomly choose the bit-rate from the set {250, ..., 250+2$n$*250}. 160 requests are assumed. From the results of different MFs and FECs in Fig. 11, we observe that the revenue decreases with the average bit-rate. The larger the bit-rate, the more spectral resources' consumption of fiber, which leads to blocked requests. A clear revenue improvement is observed by using more transmission modes, such as $\hat{\mathcal{M}}_4$ vs. $\hat{\mathcal{M}}_1$ or $\hat{\mathcal{F}}_6$ vs $\hat{\mathcal{F}}_1$. The revenue improvement ratio of $\hat{\mathcal{M}}_4$ and $\hat{\mathcal{F}}_6$ reaches about 98% and 362% when the average bit-rate increases to 1,500 Gbps, respectively.

*2) Dynamic Network:* Next, we compare the adaptive MF and multiple FEC in the scenario of dynamic traffic load. 2000 requests with a bit-rate of 250 Gbps are dynamically added and removed. The arrival time between two requests follows the exponential distribution with an average rate of $\lambda$ time-units such that the request comes as a Poisson process. The lifetime of a request follows the exponential distribution with an average rate of $\mu$ time-units. We illustrate the blocking probability for a certain network load $\mu/\lambda$ in Fig. 12. Again, the low blocking probability of $\hat{\mathcal{M}}_3$ and $\hat{\mathcal{F}}_6$ validates the benefit of using more transmission modes. An exception case is observed between $\hat{\mathcal{M}}_3$ and $\hat{\mathcal{M}}_4$ that the blocking probability of $\hat{\mathcal{M}}_4$ is higher than $\hat{\mathcal{M}}_3$. Although $\hat{\mathcal{M}}_4$ owns more flexibilities in spectrum efficiency, it also causes a higher spectrum fragmentation ratio and inefficient spectrum utilization.

## VII. Conclusion

In this paper, we studied the problem of using adaptive MFs and multiple FECs to improve the traffic provisioning in FONs. The objective is to maximize the total network revenue. To this end, we develop an MILP model and a fast two-phase heuristic algorithm, which is shown to be near-optimal for revenue maximization. Although the revenue loss is inevitable under different resource crunch scenarios, it can be improved by properly choosing the transmission mode configurations and physical parameters. Through simulations, we demonstrate that using adaptive MF enables to increase the revenue more than 100% in the scenario of high SNR while using adaptive FEC is profitable for scenarios with low SNR. While guaranteeing the revenue performance, the usage of adaptive MF configuration with PM-16QAM and multiple FEC configuration with OH 50% can be saved in the example networks. We also carry out experiments to demonstrate the case of severe resource crunch, which is simulated by increasing bit-rate and number of requests. It shows that for the case of high traffic load (large number of requests or big average bit-rate), adaptive MF takes more advantage than single MF with PM-BPSK, because it can offer more spectrum-efficient transmission modes. Further studies could be made to investigate the relationship between revenue acceptance ratio and request acceptance ratio for various revenue distributions.

## References

[1] C. Chen, F. Zhou, and S. Xiao, "Maximizing revenue with adaptive modulation and multiple FEC in flexible optical networks," in *Proc. Conf. on High Perform. Comput. and Commun. (HPCC)*, Zhangjiajie, China, Aug. 2019, pp. 2476–2481.

[2] (2018, Nov.) Cisco visual networking index: Forecast and trends, 2017-2022. [Online]. Available: https://newsroom.cisco.com/press-release-content?articleId=1853168

[3] R. B. Lourenço, M. Tornatore, C. U. Martel, and B. Mukherjee, "Running the network harder: connection provisioning under resource crunch," *IEEE Trans. Netw. Service Manag.*, Oct. 2018.

[4] Z. Zhong *et al.*, "Provisioning short-term traffic fluctuations in elastic optical networks," *IEEE/ACM Trans. Netw.*, vol. 27, no. 4, pp. 1460–1473, Aug. 2019.

[5] D. D. Le, F. Zhou, and M. Molnár, "Minimizing blocking probability for the multicast routing and wavelength assignment problem in WDM networks: Exact solutions and heuristic algorithms," *IEEE/OSA J. Opt. Commun. Netw.*, vol. 7, no. 1, pp. 36–48, Jan. 2015.
[6] K. Christodoulopoulos, I. Tomkos, and E. A. Varvarigos, "Routing and spectrum allocation in ofdm-based optical networks with elastic bandwidth allocation," in *2010 IEEE Global Telecommunications Conference GLOBECOM 2010*, Miami, FL, USA, Dec. 2010, pp. 1–6.
[7] H. Khodakarami, B. S. G. Pillai, B. Sedighi, and W. Shieh, "Flexible optical networks: an energy efficiency perspective," *IEEE/OSA J. Lightw. Technol.*, vol. 32, no. 21, pp. 3356–3367, Jun. 2014.
[8] M. Xia, M. Tornatore, C. U. Martel, and B. Mukherjee, "Service-centric provisioning in WDM backbone networks for the future internet," *IEEE/OSA J. Lightw. Technol.*, vol. 27, no. 12, pp. 1856–1865, Jun. 2009.
[9] S. K. Korotky, "Price-points for components of multi-core fiber communication systems in backbone optical networks," *IEEE/OSA J. Opt. Commun. Netw.*, vol. 4, no. 5, pp. 426–435, Jun. 2012.
[10] N. Shahriar *et al.*, "Achieving a fully-flexible virtual network embedding in elastic optical networks," in *Proc. Int. Conf. on Comput. Commun. (ICC)*, Paris, France, Apr. 2019, pp. 1756–1764.
[11] T. Koike-Akino *et al.*, "Pareto optimization of adaptive modulation and coding set in nonlinear fiber-optic systems," *IEEE/OSA J. Lightw. Technol.*, vol. 35, no. 4, pp. 1041–1049, Feb. 2017.
[12] J. Zhao, L. Yan, H. Wymeersch, and E. Agrell, "Code rate optimization in elastic optical networks," in *Proc. European Conf. on Opt. Commun. (ECOC)*, Valencia, Spain, Oct. 2015, pp. 1–3.
[13] K. Christodoulopoulos *et al.*, "Toward efficient, reliable, and autonomous optical networks: the orchestra solution," *IEEE/OSA J. Opt. Commun. Netw.*, vol. 11, no. 9, pp. C10–C24, 2019.
[14] S. Behera *et al.*, "Impairment aware routing, bit loading, and spectrum allocation in elastic optical networks," *IEEE/OSA J. Lightw. Technol.*, vol. 37, no. 13, pp. 3009–3020, Apr. 2019.
[15] K. Christodoulopoulos, K. Manousakis, and E. Varvarigos, "Offline routing and wavelength assignment in transparent WDM networks," *IEEE/ACM Trans. Netw.*, vol. 18, no. 5, pp. 1557–1570, Oct. 2010.
[16] G. Shen *et al.*, "Ultra-dense wavelength switched network: a special EON paradigm for metro optical networks," *IEEE Commun. Mag.*, vol. 56, no. 2, pp. 189–195, Feb. 2018.
[17] K. Christodoulopoulos, I. Tomkos, and E. A. Varvarigos, "Elastic bandwidth allocation in flexible OFDM-based optical networks," *IEEE/OSA J. Lightw. Technol.*, vol. 29, no. 9, pp. 1354–1366, May 2011.
[18] P. Johannisson and E. Agrell, "Modeling of nonlinear signal distortion in fiber-optic networks," *IEEE/OSA J. Lightw. Technol.*, vol. 32, no. 23, pp. 3942–3950, Oct. 2014.
[19] J. Zhao, H. Wymeersch, and E. Agrell, "Nonlinear impairment-aware static resource allocation in elastic optical networks," *IEEE/OSA J. Lightw. Technol.*, vol. 33, no. 22, pp. 4554–4564, Aug. 2015.
[20] L. Yan *et al.*, "Resource allocation for flexible-grid optical networks with nonlinear channel model," *IEEE/OSA J. Opt. Commun. Netw.*, vol. 7, no. 11, pp. B101–B108, Oct. 2015.
[21] C. Chen, F. Zhou, Y. Liu, and S. Xiao, "Throughput maximization leveraging just-enough SNR margin and channel spacing optimization," *IEEE/OSA J. Lightw. Technol.*, vol. 40, no. 13, pp. 4078–4093, Jul. 2022.
[22] P. Poggiolini, "The GN model of non-linear propagation in uncompensated coherent optical systems," *IEEE/OSA J. Lightw. Technol.*, vol. 30, no. 24, pp. 3857–3879, Dec. 2012.
[23] Yueqian. (2011, Apr.) Channel capacity with QAM inputs. (Date last accessed 15-June-2020). [Online]. Available: https://fr.mathworks.com/matlabcentral/fileexchange/31158-channel-capacity-with-qam-inputs
[24] A. Alvarado, D. J. Ives, S. J. Savory, and P. Bayvel, "On the impact of optimal modulation and FEC overhead on future optical networks," *IEEE/OSA J. Lightw. Technol.*, vol. 34, no. 9, pp. 2339–2352, Jan. 2016.
[25] L. Yan *et al.*, "Joint assignment of power, routing, and spectrum in static flexible-grid networks," *IEEE/OSA J. Lightw. Technol.*, vol. 35, no. 10, pp. 1766–1774, May 2017.
[26] G. Zervas, E. Hugues-Salas, T. Polity, S. Frigerio, and K.-I. Sato, *Node Architectures for Elastic and Flexible Optical Networks*. Cham: Springer Int. Publishing, 2016, pp. 117–157.
[27] C. Pulikkaseril *et al.*, "Spectral modeling of channel band shapes in wavelength selective switches," *Opt. Express*, vol. 19, no. 9, pp. 8458–8470, Apr. 2011.
[28] Y. Pointurier, "Design of low-margin optical networks," *IEEE/OSA J. Opt. Commun. Netw.*, vol. 9, no. 1, pp. A9–A17, Jan. 2017.
[29] A. Magnani and S. P. Boyd, "Convex piecewise-linear fitting," *Optimization and Engineering*, vol. 10, no. 1, pp. 1–17, Mar. 2009.
[30] J. Y. Yen, "Finding the k shortest loopless paths in a network," *Manag. Sci.*, vol. 17, no. 11, pp. 712–716, Jul. 1971.
[31] X. Wan, N. Hua, and X. Zheng, "Dynamic routing and spectrum assignment in spectrum-flexible transparent optical networks," *IEEE/OSA J. Opt. Commun. Netw.*, vol. 4, no. 8, pp. 603–613, Aug. 2012.
[32] M. Ju, F. Zhou, Z. Zhu, and S. Xiao, "Distance-adaptive, low CAPEX cost *p*-cycle design without candidate cycle enumeration in mixed-line-rate optical networks," *IEEE/OSA J. Lightw. Technol.*, vol. 34, no. 11, pp. 2663–2676, Apr. 2016.
[33] P. Poggiolini *et al.*, "The LOGON strategy for low-complexity control plane implementation in new-generation flexible networks," in *Proc. Opt. Fiber Commun. Conf. (OFC)*, 2013, p. OW1H.3.
[34] F. Zhou, J. Liu, G. Simon, and R. Boutaba, "Joint optimization for the delivery of multiple video channels in Telco-CDNs," *IEEE Trans. Netw. Service Manage.*, vol. 12, no. 1, pp. 87–100, Mar. 2015.

**Cao Chen** received the B.S. degree from the University of Electronic Science and Technology of China, Chengdu, China, in 2015. He is currently working toward the joint Ph.D. degree with Shanghai Jiao Tong University, Shanghai, China, and Avignon University, Avignon, France.

**Fen Zhou** (Senior Member, IEEE) received the Ph.D. degree from Institut National des Sciences Appliquées de Rennes, Rennes, France, in 2010, and the HDR degree from Avignon University, Avignon, France, in 2018. He is a Full Professor with IMT Nord Europe, Institut Mines-Télécom, France. Prior to that, he was an Associate Professor with LIA lab, Avignon University from 2012 to 2018, and with the Institut Supérieur d'Electronique de Paris, Paris, France, till August 2020. His research interests include network survivability and security, routing and resource allocation, and network function virtualization. In the past ten years, he has coordinated or co-coordinated several research projects in the national or international levels, such as PHC Cai Yuanpei, Campus France Eiffel Scholarship, Science Sans Frontiers, Campus France Profas B+, PACA Regional project, LIA lab project, Open project of Shanghai Jiao Tong University, Shanghai, China. He has also been involved in the French Beyond 5G project, European FP7 CNG project, Zewall project, and Vaucluse @muse project.

**Massimo Tornatore** (Senior Member, IEEE) is currently an Associate Professor with Politecnico di Milano, Milan, Italy. He was an Adjunct Professor with the University of California, Davis, CA, USA, and a Visiting Professor with the University of Waterloo, Waterloo, ON, Canada. He has coauthored more than 400 peer reviewed conference and journal papers, two books, and one patent in his research areas, which include performance evaluation, optimization and design of communication networks, with an emphasis on the application of optical networking technologies, cloud computing, and machine learning application for network management. He was the recipient of the 19 best paper awards. He is a member of the Editorial Board of IEEE COMMUNICATION SURVEYS AND TUTORIALS, IEEE COMMUNICATION LETTERS, *Springer Photonic Network Communications*, and *Elsevier Optical Switching and Networking*.

**Shilin Xiao** received the M.S. degree from the University of Electronic Science and Technology of China, Chengdu, China, in 1988, and the Ph.D. degree from Shanghai Jiao Tong University (SJTU), Shanghai, China, in 2003. From 1988 to 1999, he was with the Guilin Institute of Optical Communications. Since 2000, he has been with the State Key Laboratory of Advanced Optical Communication Systems and Network, SJTU, where he is currently a Professor. He has authored or coauthored more than 100 papers in technical journals and conferences. His main research interests include optical communications, especially optical switching, and passive optical networks. He is a Senior Member of the Chinese Institute of Electronics and Optical Society of China.